

High energy emission from extended region within the blazar jet during quiet gamma-ray state

Piotr Banasinski*

Department of Astrophysics, The University of Lodz, ul. Pomorska 149/153, 90-236 Lodz, Poland,

E-mail: p.banasinski@uni.lodz.pl

Wlodek Bednarek

Department of Astrophysics, The University of Lodz, ul. Pomorska 149/153, 90-236 Lodz, Poland,

E-mail: bednar@astro.phys.uni.lodz.pl

During the quiet γ -ray state of blazars the high energy emission is likely to be produced in the extended part of the inner jet in which the conditions can change significantly. Therefore, homogeneous SSC model is not expected to describe correctly the quiet state emission features. We consider inhomogeneous synchrotron self-Compton (SSC) model for the large part of the inner jet in which synchrotron and IC emission of relativistic electrons is taken into account self-consistently by applying the Monte Carlo method. The results of calculations are compared with the observation of BL Lac object Mrk 421 in the low state.

*The 34th International Cosmic Ray Conference,
30 July- 6 August, 2015
The Hague, The Netherlands*

*Speaker.

1. Introduction

Observations of BL Lacs with the modern Cherenkov observatories and Fermi-LAT telescope clearly identifies persistent low level emission lasting for months [1]. Future high energy observations (e.g. CTA) should allow detailed spectral studies of blazars in the low, steady emission state. Such persistent emission can not be explained in terms of the homogeneous blob model since during the time scale of a month the parameters in the moving blob should change drastically.

We discuss the inhomogeneous SSC model for the blazar emission assuming that the steady emission is produced in the large region of the inner jet that extends from the distance of several Schwarzschild radius up to a parsec scale.

2. Inhomogeneous jet model

We consider self-consistent scenario for production of synchrotron and IC radiation in term of SSC for the inhomogeneous jet with constant opening angle α . In our model we assume that the plasma in the jet moves along with the constant Lorentz factor Γ_j . It is assumed that the outflow of the plasma along the jet is stationary. Electrons are accelerated in the jet to maximum energies determined by the balance between acceleration energy gains and energy losses on synchrotron radiation. The synchrotron energy losses of electrons are determined by the value of the magnetic field $B(x)$ at the distance x from the base of the jet. Electrons accelerated at the distance x along the jet comptonize the synchrotron radiation produced locally in a specific part of the jet. As a result, γ -ray photons are produced in the SSC process. γ -rays, produced inside the jet, can be partially absorbed when propagating through the outer parts of the jet. Electrons accelerated at specific distance lose their energy only partially and move to the outer parts of the jet (i.e. to subsequent layers). In order to perform numerical calculations, we divide the the conical jet on several slabs with the constant thickness in \log scale $\Delta(\log x)$. It is assumed that the conditions at every slab are constant (efficiency of electron acceleration, magnetic field strength etc.) but they change with the distance from the base of jet, as it is described below. All calculations are done in the plasma rest frame.

2.1 Specific model parameters

We assume that electrons are accelerated continuously in the range of distances along the jet from $x_{\min} = 10R_s$ up to $x_{\max} = 10^5 R_s$. Electrons are cooled up to $x_{\text{end}} = 10^6 R_s$, where $R_s \approx 3 \times 10^{13} M_8 \text{ cm}$ is a Schwarzschild radius, $M_{\text{BH}} = 10^8 M_8 M_\odot$ is the black hole mass in units of the Solar mass M_\odot . Electrons produce synchrotron radiation in the magnetic field of the jet. It is expected that the toroidal component of the magnetic field in the conical jet follows a simple scaling, $B \propto r^{-1}$, then we estimate it by

$$B(x) = \frac{B_{\text{in}} r_{\text{in}}}{r_j(x)}, \quad (2.1)$$

where B_{in} is the strength of the toroidal component of the magnetic field in G at the base of the jet, r_{in} is the inner radius of the jet at the base and $r_j(x) = r_{\text{in}} + \alpha x$ is the radius of the slab at the distance x . The inner radius of the jet is related to the Schwarzschild radius, $r_{\text{in}} = 3 \times R_s \text{ cm}$.

2.2 Acceleration and cooling of electrons

The details of acceleration process of relativistic electrons in the jet are not clear at present. Therefore, we consider simple scenario in which electrons are injected with similar power along the jet axis according to, $dL_e/dx = L_e/(x_{\max} - x_{\min})$, where L_e is the power taken by relativistic electrons from the jet. Such injection scenario for relativistic electrons could occur in the case of the acceleration process related to the energy content of the jet plasma, i.e shock acceleration mechanism.

The acceleration time scale of electrons at a specific distance from the base of the jet can be parametrized by the acceleration efficiency according to $\tau_{\text{acc}} = R_L/\eta c \approx 1.1 \times 10^3 E_{\text{TeV}} \eta_{-4}^{-1} B^{-1}$ s, where $R_L = E_e/qB$ is the Larmor radius of accelerated particles, $E_e = 1 E_{\text{TeV}}$ TeV is the electron energy, c is the velocity of light and B is a magnetic field strength in Gauss. The acceleration coefficient is $\eta = 10^{-4} \eta_{-4}$. The cooling time scale of electrons on synchrotron process is equal to $\tau_{\text{syn}} = E_e/\dot{E}_{\text{syn}} \approx 4.0 \times 10^2 B^{-2} E_{\text{TeV}}^{-1}$ s, where $\dot{E}_{\text{syn}} = 4/3c\sigma_T U_B \gamma_e^2$, σ_T is the Thomson cross section, U_B is the energy density of the magnetic field and γ_e is the Lorentz factor of electron. By comparing the acceleration time scale and the synchrotron cooling time scale, we estimate the maximum energies of electrons to which they are accelerated, $\gamma_{\max} \approx 1.2 \times 10^6 \eta_{-4}^{1/2} B^{-1/2}$. Note that electrons with such energies produce characteristic synchrotron photons with the maximum energies, $\varepsilon \approx 0.5 m_e c^2 (B/B_{\text{cr}}) \gamma^2$ ($B_{\text{cr}} \approx 4.4 \times 10^{-13}$ G is a critical magnetic field), extending up to $\varepsilon_{\max} \approx 8 \eta_{-4}$ keV. If the acceleration efficiency does not depend on the distance from the base of the jet, then the cut-off in synchrotron spectrum should be also independent on the location of the acceleration region in the jet.

We assume that electrons gain energy from turbulent plasma of the jet reaching the differential power law spectrum which can be expressed per unit length of the jet and unit time interval as $dN_e/dE_e dx dt = N_e E_e^{-\beta}$ (el. $\text{s}^{-1} \text{GeV}^{-1} \text{cm}^{-1}$), where N_e is the normalization factor and β is the spectral index. N_e is determined by normalizing this electron injection spectrum to the total energy in relativistic electrons at a specific distance from the base of the jet,

$$\frac{dL_e}{dx} = N_e \int_{E_{\min}}^{E_{\max}} E_e^{-\beta} E_e dE_e, \quad (2.2)$$

where E_{\min} is the minimum energy of relativistic electrons fixed on 1 GeV for normalise puposes.

Electrons lose energy on the synchrotron and inverse Compton processes in every slab. The time needed to pass through the slab is equal to $\tau_{\text{dyn}} = \Delta x/\beta_j c \approx \Delta x/c$ s, where $\beta_j c$ is the velocity of the plasma in the jet. We assume that after this time electrons are transferred to the upper slab.

2.3 Synchrotron and IC radiation from electrons

The differential density of synchrotron photons, $n_{\text{syn}}(x)$, at the distance x from the base of the jet is estimated by multiplying the synchrotron emissivity of electrons injected within dx , $j_{\text{syn}}(x)$ by the characteristic time spend by the synchrotron photon in the jet, $r_j(x)/c$ and dividing by the cross-section of the jet, $\pi r_j(x)^2$. As an example, we show the differential photon density produced by electrons in the jet as a function of distance from the base of the jet in Fig. 1a, for some characteristic parameters of the jet. Note that the energy density of synchrotron photons drop with the distance from the base of the jet.

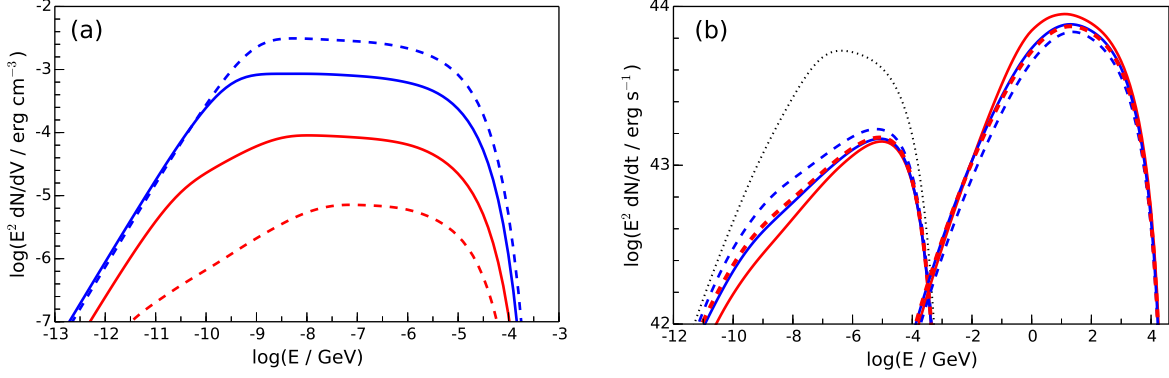


Figure 1: (a) Differential synchrotron photon density (0th generation, multiplied by energy squared) produced at different distances from the base of the jet, $x = 10^{15}$ cm (blue dashed curve), 10^{16} cm (blue solid), 10^{17} cm (red solid) and 10^{18} cm (red dashed). The parameters describing the jet are the following: $B_{\text{in}} = 10$ G, $\eta = 10^{-4}$, $\beta = 2$, $L_e = 10^{43}$ erg s $^{-1}$ and $M_{\text{BH}} = 3 \times 10^8 M_{\odot}$. (b) The spectral energy distribution for the synchrotron and IC γ -ray spectra produced in the 0th generation (black dotted curve), the 1st generation (red solid curves), the 2nd generation (blue dashed), the 3rd (blue solid) and 5th (red dashed). The parameters of the model are: $B_{\text{in}} = 10$ G, $\eta = 10^{-3}$, $\beta = 2$, $L_e = 10^{45}$ erg s $^{-1}$ and $M_{\text{BH}} = 3 \times 10^8 M_{\odot}$.

The calculation of the IC γ -ray spectrum produced by electrons, that are also responsible for synchrotron energy losses, is not straightforward since the background radiation is produced by this same population of electrons. So then, electrons injected into the specific volume filled with the magnetic field compete between losing energy on both processes. Only when the background radiation field (depends on the electron equilibrium spectrum) is well defined then the IC γ -ray spectra can be easily calculated by applying the standard formula for the γ -ray spectrum from mono-energetic electrons in [2]. We define the radiation field at a specific location in the jet in the way described in detail in the next section.

2.4 Method to calculate multiwavelength spectra

The energy lost by electrons on the synchrotron process and IC process in the far Thomson regime is subtracted continuously from the electron. But, in the Klein-Nishina regime, and close to the border between Thomson and Klein-Nishina regimes, the electron loses its energy in discrete amounts. In order to consider self-consistently the energy losses of electrons on synchrotron and Inverse Compton process (and produced by them multifrequency spectrum), we apply the iteration method. At first, we only calculate the synchrotron spectrum produced by injected electrons, assuming that they lose energy only on a synchrotron process (so called 0-th generation synchrotron spectrum). In the next generations, injected electrons lose energy on the synchrotron process and on the IC process by scattering photons from the previous generation of synchrotron spectrum. Based on such procedure, we calculate the next generations of synchrotron and IC spectrum.

As an example, we calculate the synchrotron and the IC spectra produced in the jet for the specific set of parameters in specific generations. We present the results on Fig 1b. The 0th generations synchrotron spectrum is higher than spectra from forward generations because electrons lose energy only for synchrotron process. The differences between spectra from further generations become smaller and the computed synchrotron and IC spectra tend to the steady state. Note that the synchrotron and IC spectra calculated already in the 3rd generation saturate nicely. Therefore,

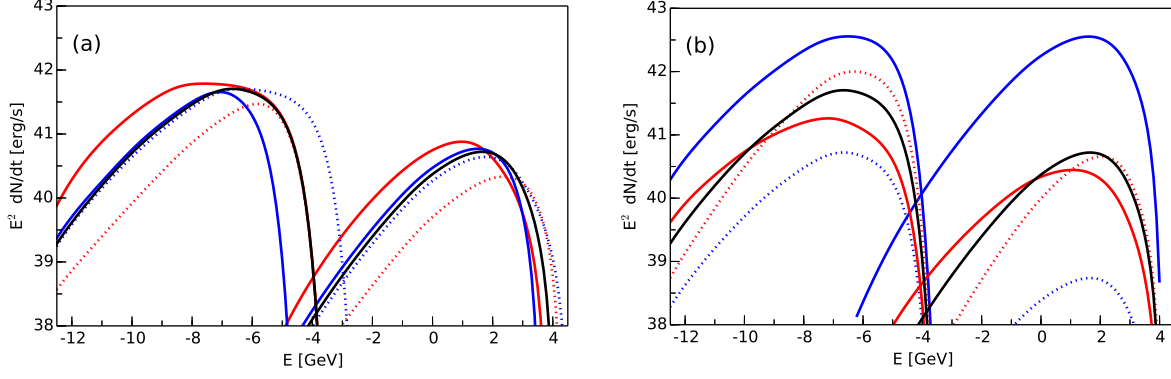


Figure 2: The synchrotron and IC spectrum energy distribution (SED) calculated in terms of the inhomogeneous SSC model as a function of parameters describing the model. (a) For different values of the magnetic field strength and the acceleration coefficient of electron: $B_{\text{in}} = 10$ G and $\eta = 10^{-4}$ (black solid curve), $B_{\text{in}} = 3$ G (red dotted), $B_{\text{in}} = 30$ G (red solid), $\eta = 10^{-3}$ (blue dotted), and $\eta = 10^{-5}$ (blue solid). (b) For different values of the power in electrons and spectral index of injected electrons: $L_e = 10^{43}$ erg s $^{-1}$ and $\beta = 2.0$ (black solid), $L_e = 10^{42}$ erg s $^{-1}$ (blue dotted), $L_e = 10^{44}$ erg s $^{-1}$ (blue solid), $\beta = 1.7$ (red dotted) and $\beta = 2.3$ (red solid). The other parameters, unless otherwise noted, are: $B_{\text{in}} = 10$ G, $L_e = 10^{43}$ erg s $^{-1}$, $\eta = 10^{-4}$, $\beta = 2$, and $M_{\text{BH}} = 10^8 M_{\odot}$.

we conclude that the 3rd generation spectra provide self-consistent solution of the cooling process of electrons on the synchrotron and IC radiation processes locally in the jet.

2.5 The example of multiwavelength spectra

In this section we investigate how the synchrotron and IC spectra depend on the basic parameters of the inhomogeneous SSC jet model. The results of our calculations for various parameters are shown on Fig. 2.

The essential parameters of our inhomogeneous model are the acceleration coefficient η of electrons and strength of magnetic field in the base of the jet B_{in} . The spectra for different value of B_{in} and η are presented on Fig. 2a. For the strong magnetic field, the synchrotron spectra are broader and the peak in the IC spectrum is at relatively low energies (GeV range). The acceleration coefficient of electrons affect their maximum energies. If η is large, then the cut-offs in the synchrotron and IC spectrum are shifted to higher energies.

The dependence of the power in relativistic electrons L_e and the spectral index β on the spectra are investigated if Fig 2b. As expected, the level of the synchrotron and IC spectra increase with the power in electrons. The shape of the synchrotron and IC spectra and the location of the peak depends mainly on the spectral index β . The harder spectra are produced by electrons with lower β .

3. Internal absorption of γ -rays in the jet

γ -rays produced in the inner part of the active region in the jet have to propagate through the synchrotron radiation produced in the outer parts of the jet. We calculate the optical depth for γ -rays ($\gamma - \gamma \rightarrow e^{\pm}$), originated at specific distance x from the base of the jet, in the synchrotron radiation produced by electrons at larger distances by integrating the cross section for $\gamma - \gamma \rightarrow e^{\pm}$ [3] over the propagation distance up to x_{end} . It is assumed that γ -rays are injected at small angles

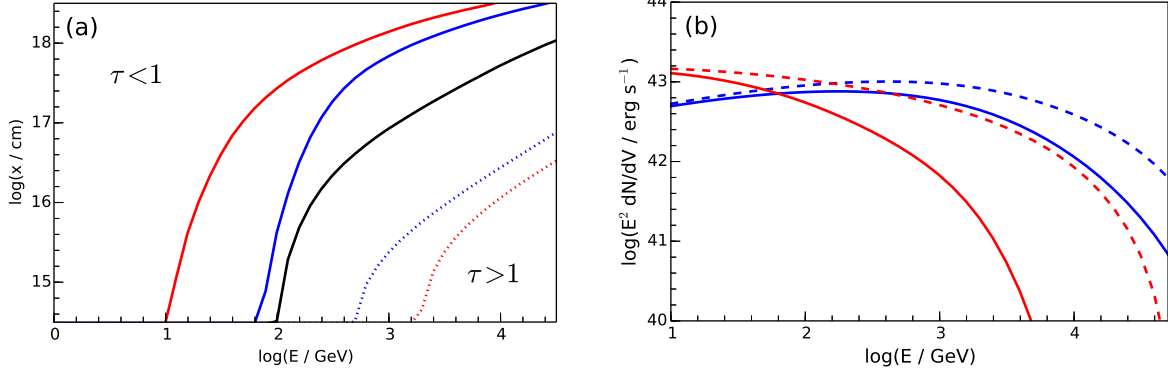


Figure 3: (a) Relation between energy and injection place of γ -rays for the optical depth equals unity. The parameters of the model are: $B_{\text{in}} = 3 \text{ G}$ and $L_e = 10^{43} \text{ erg s}^{-1}$ (blue dotted curve); $B_{\text{in}} = 30 \text{ G}$ and $L_e = 10^{43} \text{ erg s}^{-1}$ (blue solid); $B_{\text{in}} = 10 \text{ G}$ and $L_e = 10^{43} \text{ erg s}^{-1}$ (black solid); $B_{\text{in}} = 10 \text{ G}$ and $L_e = 10^{42} \text{ erg s}^{-1}$ (red dotted); $B_{\text{in}} = 10 \text{ G}$ and $L_e = 10^{44} \text{ erg s}^{-1}$ (red solid). The other parameters, are: $\eta = 10^{-4}$, $\beta = 2$, and $M_{\text{BH}} = 3 \times 10^8 M_{\odot}$. (b) The comparison of γ -ray spectra produced in the jet (dashed curves) and partially absorbed in the synchrotron radiation in the outer regions of the jet (solid curves) for two values of magnetic field strength: $B_{\text{in}} = 3 \text{ G}$ (red lines) and $B_{\text{in}} = 30 \text{ G}$ (blue lines). The other parameters are: $L_e = 3 \times 10^{44} \text{ erg s}^{-1}$, $\eta = 10^{-2}$, $\beta = 2$, and $M_{\text{BH}} = 3 \times 10^8 M_{\odot}$.

to the jet axis, i.e. close or smaller than the opening angle of the jet α . In such a case, γ -rays propagate within the jet volume filled with synchrotron radiation. In our calculations we apply the standard formula for the reciprocal of the mean interaction length for photon-photon e^{\pm} pair production (e.g. [4]). We assume that synchrotron radiation, produced locally in the rest frame of the jet at the distance x , is isotropic but the differential density of synchrotron photons depends on the distance from the base of the jet.

In Fig. 3a we show the distance at which produced γ -rays with different energy are efficiently absorbed. Even small change of the power in relativistic electrons or magnetic field strength lead to a large change of the optical depth in the jet. We conclude that in bright BL Lacs internal absorption should be important if the plasma in the jet does not have a very large Doppler factor. In Fig. 3b we show real effect of internal absorption on γ -ray spectra for two sets of the model parameters.

4. Application to the quiescent state of Mrk 421

As an example we interpret the quiescent state of multiwavelength emission from well known BL Lac Mrk 421. The broad band spectra of this source have been nicely measured in the quasi-simultaneous observational campaigns that was able to cover the whole energy range (from the radio to TeV γ -rays). For the first time the γ -ray energy range has been completely covered by the Fermi and the MAGIC telescopes in campaigns [1].

We selected the black hole mass of Mrk 421 in the way to be consistent with the results of observations. It has been fixed on $3 \times 10^8 M_{\odot}$ which is in the range from $(2 - 9) \times 10^8 M_{\odot}$ [5, 6]. The electrons are injected into the jet with the simple power law spectrum with spectral index 2.1. and are accelerated locally in the jet with the constant acceleration efficiency ($\eta = 1.5 \times 10^{-5}$). This value is constrained by the cut-off energy in the observed synchrotron spectrum from Mrk 421. Moreover, the shape and place of the cut-off in observed IC spectrum allow us to constrain the magnetic field strength ($B_{\text{in}} = 10 \text{ G}$). The power in electrons can be estimated by comparing

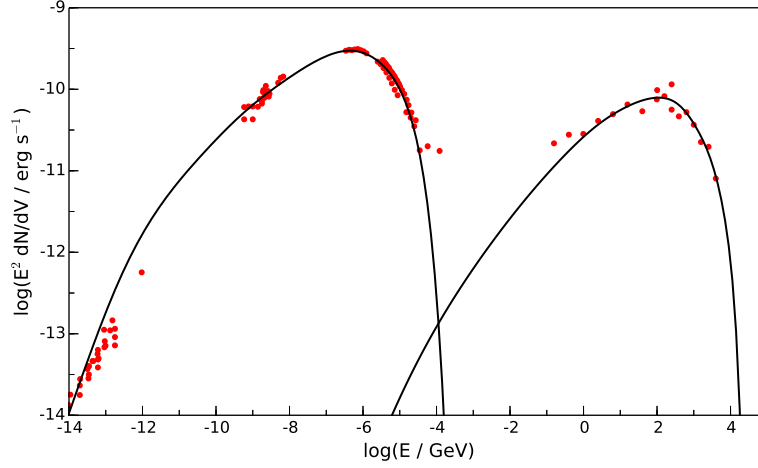


Figure 4: The comparison of multiwavelength spectrum (SED), observed during the quiescent state from Mrk 421 [1], with the spectrum calculated in terms of the self-consistent inhomogeneous extended jet SSC model with constant injection rate of electrons. The parameters of the model are the following, $B_{\text{in}} = 10$ G, $\eta = 1.5 \times 10^{-5}$, $\beta = 2.1$, $L_e = 1.9 \times 10^{43}$ erg s $^{-1}$, $M_{\text{BH}} = 3 \times 10^8 M_{\odot}$, and the Doppler factor of jet plasma $D_j = 5.7$.

levels of the synchrotron and the IC bump ($L_e = 1.9 \times 10^{43}$ erg/s). Next, we find that the Doppler factor for Mrk 421 is equal $D_j = 5.7$ what agree well with estimated values for this BL Lacs (radio observation suggest that Doppler factor is the order of few, e.g. [7]).

In the end, we take into account the absorption of γ -rays from the jet during their propagate to the observer. γ -rays, which leave the jet, propagate through the extragalactic background light (EBL). They can be absorbed by pair production ($\gamma + \gamma \rightarrow e^{\pm}$) if the threshold condition is fulfilled. Efficiency of absorption depends on the distance between observer and γ -ray source. Even for nearby objects like Mrk 421, with $z = 0.031$, the absorption effect is not negligible. To calculate the optical depth for γ -rays, we use semi-analytical model presented in [8].

In Fig 8 we show the spectrum, calculated for above parameters, after taking account internal absorption effects in the jet and on the EBL. Computed spectra are compared with multiwavelength observations of low level emission state.

5. Conclusion

We develop the inhomogeneous SSC jet model for BL Lacs objects in low, steady emission state. The model include the absorption of γ -rays on the synchrotron photons in the jet and on the EBL. We successfully adapt our model to near BL Lac object Mrk 421. The model requires the relativistic boosting of emission with Doppler factor of a few, which agree with the radio observations of BL Lacs jet. We find that for a certain sets of parameters, the internal absorption in the jet is significant, especially for luminous blazars. As the next step, we are planning to add some modifications to our code like e.g. taking account cascades in the jet initiated by electrons.

References

- [1] Abdo, A.A. et al. 2011 ApJ 736, 131
- [2] Blumenthal, G.R., Gould, R.J. 1970 Rev.Mod.Phys. 42, 237

- [3] Jauch, J.M., Rohrlich, F. 1955, *The Theory of Photons and Electrons*, Addison-Wesley
- [4] Bednarek, W, Protheroe, R.J. 1999 *MNRAS* 310, 577
- [5] Wu, X.-B., Liu, F. K., Zhang, T. Z. 2002 *A&A*, 389, 742
- [6] Barth, A. J., Ho, L. C., Sargent, W. L. W. 2003 *ApJ*, 583, 134
- [7] Lico, R., Giroletti, M., Orienti, M., et al. 2012, *A&A*,545, A117
- [8] Gilmore, R. C., Somerville, R. S., Primack, J. R., Dominguez, A. 2012, *MNRAS*, 422, 3189.